Cement & Concrete Composites 35 (2013) 71–77

Contents lists available at SciVerse ScienceDirect

Cement & Concrete Composites

journal homepage: www.elsevier.com/locate/cemconcomp

Effect of polymers on cement hydration: A case study using substituted PDADMA

D. Jansen [a], F. Goetz-Neunhoeffer [a,*], J. Neubauer [a], R. Haerzschel [b], W.-D. Hergeth [b]

[a] Mineralogy, GeoZentrum Nordbayern, University of Erlangen-Nuremberg, D-91054 Erlangen, Germany
[b] Wacker Chemie AG, Muenchen, Germany

ARTICLE INFO

Article history:
Received 30 November 2011
Received in revised form 23 August 2012
Accepted 24 August 2012
Available online 5 September 2012

Keywords:
Cement hydration
PDADMAC
Calorimetry
Quantitative XRD-analysis

ABSTRACT

A study was carried out, using heat flow calorimetry and quantitative X-ray diffractometry, of the different influences which are exerted by types of cationic Polydiallyldimethylammonium (PDADMA) displaying different anionic counterions on the hydration behavior of an Ordinary Portland Cement (OPC). It was shown that the influence of the cationic polymer PDADMA on the hydration of the cement will tend to be strongly dependent on the nature of the anionic counterion. In case of OH^-, more calcium sulfate will tend to be dissolved in the early stages, which acts in turn as an accelerator for the hydration of the C_3S phase. In case of SO_4^{2-} there will tend to occur a secondary gypsum precipitation, which will in turn act to lower the Ca^{2+} – content in the mix water, leading to a retardation of the hydration process compared to the hydration in absence of polymer.

1. Introduction

The hydration of OPC is still a live scientific issue and the object of much controversy and debate. Many different methods of examination have been applied in the attempt to clarify the hydration process. The very complex processes of cement hydration have already been reviewed elsewhere [2,3]. One of the most important issues of research is to explain the kinetics of hydration, which can be expressed in terms of heat flow diagrams [2–5,43,44] and is separated into initial period (I), induction period (II), acceleration period (III) and deceleration period (IV) (Fig. 1). The acceleration period and the deceleration period are often treated as a single period and referred to as "the main period". Very often, an additional heat flow maximum becomes visible during the deceleration period of cement hydration. Since our research is focused on the "main hydration" period within the hydration process as a whole, we call the maximum which occurs at about 7.5 h the "first maximum", and the heat flow which occurs at about 15 h (sulfate depletion peak) the "second maximum". This "second maximum" has already been described by Lerch and called "sulfate depletion peak" [25].

The phase development of cements during hydration can be traced by means of X-ray diffraction [4,5]. Heat flow curves and data from XRD experiments can be combined and the early heat flow during cement hydration can be related to different specific reactions.

Polymers are very important means to the adjustment of the properties of a number of concrete products, such as self-compacting concrete and ultra high performance concrete (UHPC). Modern dry mortar technology is also unthinkable without functional polymers [1]. In addition to having other applications, superplasticizers are added to dry mortars to reduce water content and to adjust self leveling properties for self leveling underlayments (SLU). Redispersible polymer powders are nowadays the favored organic binder component in dry mortars to increase properties such as adhesion to the substrate, abrasion resistance, flexibility and also workability and cohesion of the fresh mortar.

When developing and manufacturing dry mortars it is always an important issue to know whether the polymers and additives have an impact on the hydration process of the inorganic binders which are used. Specific knowledge of the interaction between polymers and other additives, and of hydration reactions of cementitious systems, might also be important in order to understand an unsatisfactory performance of cementitious products in application, e.g. their setting too quickly, or an unintended retardation. This is the reason why the influence of different polymers has already been examined by numerous authors and has also been reviewed [e.g. [30].

Plank et al. [26,27] investigated the influence of superplasticizers as well as anionic and cationic latexes on the hydration behavior of Portland cements, measuring zeta potentials and adsorption isotherms. It was shown that the charged latex particles adsorb (Langmuir type adsorption) selectively on the surfaces of those hydrating cement particles which display an opposite charge. Additionally it was shown that the anionic latexes adsorb a considerable amount of Ca^{2+} from the pore solution. Larbi and Bijen [28]

* Corresponding author. Tel.: +49 9131 85 25780; fax: +49 9131 85 23734.
E-mail address: goetz.gzn@me.com (F. Goetz-Neunhoeffer).

0958-9465/$ - see front matter © 2012 Elsevier Ltd. All rights reserved.
http://dx.doi.org/10.1016/j.cemconcomp.2012.08.022

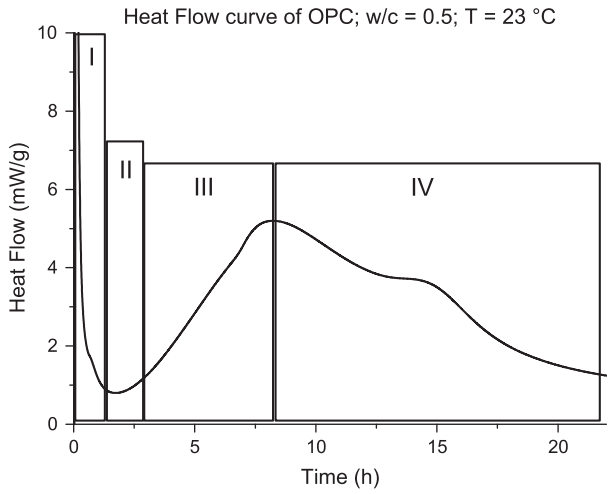

Fig. 1. Typical heat flow curve of an OPC.

examined the pore solution during cement hydration and the influence of different polymers on the composition of the pore solution. They showed that there is an interaction between polymers and ions (Ca^{2+}, SO_4^{2-}, OH^-) released by the cement during hydration. The carboxylic groups of the polymer appear to interact with the positive Ca^{2+} in pore solution. Su et al. [29] worked out that acrylic polymers tend to retard cement hydration and related this retardation either to the formation of a skin of the polymer around the cement grains, which then acts to restrict water access, or to the interaction of the polymers with Ca^{2+} from the pore solution. The interaction between cement hydration and ethylene/vinyl acetate copolymers (EVA) has been investigated in detail by Silva et al. [31–34]. There was discovered to be an interaction between the ester groups of the polymer and Ca^{2+} from the pore solution, resulting in the formation of calcium acetate and therefore a retardation of the cement hydration. Moreover, the amount of portlandite was discovered to decrease where EVA is added, due to the consumption of Ca^{2+} by the polymer [31]. Additionally, an investigation was made, using X-ray transmission microscopy, of the hydration of C_3A under addition of EVA [32]. It was shown that EVA changes the morphology and kinetics of ettringite precipitation. The reaction of C_3A in calcium hydroxide–gypsum saturated solution is retarded by the presence of EVA. The dissolution of C_3S was also found to be hindered when adding EVA [33]. It was discussed that EVA releases CH_3COO^- into the pore solution which in turn interacts with Ca^{2+}. In addition, it was also discussed whether polymer particles might possibly act as a nucleation site for the C–S–H phase [34]. The fact that polymer modification influences cement hydration and cement microstructure was also described by Dimmig-Osburg et al. [35]. It was shown that polymer modification delays and slows the reaction of the clinker phases, alternatively the precipitation of ettringite and C–S–H phase.

Polymers of type PDADMA are very interesting to control and optimize workability of highly flexible tile adhesives, which then contain very high amounts of polymer. But PDADMA with counterion Cl^-, which is applied successfully for waste water treatment, might be problematic for cement application and therefore PDADMA with counterion OH^- and SO_4^{2-} were chosen for this investigation.

In this work heat flow curves of OPC hydration with addition of different polymers of type PDADMA with counterion OH^- and SO_4^{2-} are calculated from quantitative XRD-data and enthalpy of reaction data. The comparison of calculated with the experimental heat flow is used to enable detailed insight in early OPC hydration, especially on alite, C_3A and calcium sulfates dissolution respectively precipitation of C–S–H, portlandite and ettringite.

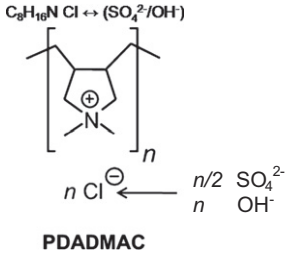

Fig. 2. Structure of Polydiallyldimethylammonium chloride (PDADMAC).

2. Materials and methods

Polydiallyldimethylammonium chloride (PDADMAC), a homopolymer of diallyldimethylammonium chloride, is a cationic polymer with a high charge density and with a molecular weight of hundreds of thousands of grams per mole. PDADMAC is synthesized by radical polymerization and is soluble in water. The counterion to the positive charge of the nitrogen is chloride. PDADMAC is mainly employed in the papermaking process, inasmuch as it can be used in order to control disturbing substances. In addition to this, PDADMAC can be used as an organic coagulant in waste water treatment. Another interesting use of PDADMAC is its use in dry mix mortar technology [6]. For our experiments, the counterion Cl^- at PDADMAC was substituted for both OH^- and SO_4^{2-}. The structure of PDADMAC is shown in Fig. 2.

The PDADMAC has a molecular weight of appr. $M_w \sim 200{,}000$ g/mol and a chlorine content of 20.3%.

A 100 g aqueous PDADMAC solution of 41.4% total solids was charged to a dialysis membrane tubing DTV12000.05.000 (Medicell International Ltd.; London) having a pore width corresponding to $M_w \sim 12{,}000$–$14{,}000$ Daltons. This tubing was placed in a glass beaker containing 3 L of a 1 M solution of either NaOH or Na_2SO_4 for 14 days of equilibration without stirring.

Data of the PDADMA-X solutions after dialysis, along with the original PDADMAC solution, are summarized in Table 1. The elemental composition represents the total ion concentrations of the PDADMA-X polyelectrolyte solutions (i.e. at equilibrium dissociation).

The polymer used was dissolved in the water which was mixed with the cement when starting the experiments. In our experiments we made use of 2 wt.% of polymer in proportion to the amount of cement in order to get clear information on their influence.

Heat flow experiments were performed using a commercial TAM Air calorimeter. The cement was mixed and prepared into a sample holder in an air-conditioned room at a temperature of 23 °C. The sample holder was then placed in the calorimeter and the heat flow was measured and plotted over time. Because of the disturbance of the signal when opening the calorimeter, the

Table 1
Characterization of the PDADMA-X used.

	Cl (g/100 g polymer)	S (g/100 g polymer)	Na (g/100 g polymer)
PDADMAC	20.3	–	–
PDADMA-OH	2.5	–	16.1
PDADMA-SO_4	2.0	17.8	21.1

Table 2
Mineralogical and chemical composition of the OPC used.

Phase	wt.%	Oxide	wt.%
Alite (C_3S)	57.7 ± 1.2	CaO	66.2
Belite (C_2S)	11.7 ± 0.6	SiO_2	22.6
α'-C_2S	8.0 ± 0.5	Al_2O_3	4.1
C_3A_{cubic}	5.6 ± 0.3	Fe_2O_3	1.3
$C_3A_{orthorombic}$	4.8 ± 0.3	MgO	0.8
C_4AF	1.9 ± 0.2	K_2O	0.7
Gypsum	0.8 ± 0.1	Na_2O	0.1
Bassanite	1.5 ± 0.1	SO_3	3.4
Anhydrite	3.0 ± 0.2	LOI	0.8
Calcite	2.2 ± 0.2		
Quartz	0.9 ± 0.1		
Arcanite	0.9 ± 0.1		
Amorphous/misfitted	1.0 ± 0.5		

first 30 min of the signal have to be interpreted with care. Since our research focuses on the main hydration process of the cement between 2.5 and 22 h this just-mentioned disturbing influence on the recorded data does not affect our interpretation.

The OPC used was a commercial CEMI 52.5 R which is commonly used in dry mix mortar technology. The phase composition, which was derived from Rietveld analysis (applying the *G*-factor method presented later in this manuscript), as well as the chemical composition, are shown in Table 2. A detailed discussion about the amorphous content of the investigated OPC can be found elsewhere [8].

The method used for the quantification of the XRD pattern of the hydrating cement pastes was a Rietveld refinement [9] employing a fundamental parameter approach [39] and using the Rietveld software Topas V4.0. The external standard method used was based on the suggestion of O'Connor and Raven, using a calibration factor (in our case called *G*) in order to calculate absolute quantities [7,8].

The special problem when using X-ray diffraction in OPC pastes is the fact that the C–S–H phase and the water cannot be quantified directly by means of X-ray. In addition, it can also happen that the AFm phase precipitates with a quite low degree of crystallinity, which makes determination of precise quantities very difficult.

The use of Rietveld software for the quantification of XRD diagrams has the disadvantage that the results are normalized to 100 wt.% so that there is a falsification of the data as soon as amorphous or misfitted phases prove to be present in the cement paste.

Therefore an adequate method, based on an internal or external standard, should be employed for the quantification of cement pastes. It has been shown that the *G*-factor method which was first described by O'Connor and Raven [7] is the most suitable method for the quantification of hydration reactions [5].

This method involves the calibration of the diffractometer with a well known standard (in our case silicon powder derived from milling of a single crystal). A calibration factor *G* is calculated using following equation:

$$G = S_{Si}\frac{\rho_{Si}V_{Si}^2\mu_{Si}^*}{C_{Si}} \quad (1)$$

where S_{Si} is the Rietveld scale factor of silicon from Rietveld analysis; ρ_{Si} the density of silicon; V_{Si} the unit-cell volume of silicon; C_{Si} the Weight fraction of silicon (100 wt.%); μ_{Si}^* the mass attenuation coefficient of silicon.

The factor *G* is then used in order to calculate the quantity of each single phase in the cement paste, taking into account the density of each phase *j* (ρ_j), the unit-cell volume of each phase *j* (V_j), the scale factor calculated from Rietveld refinement for each phase *j* (s_j) and the mass attenuation coefficient of the whole sample (μ_{SAMPLE}^*).

Table 3
Structures used for Rietveld-refinement.

Phase	ICSD Code	Reference
Alite (C_3S)	94742	De La Torre et al. [11]
Belite (C_2S)	963	Jost et al. [12]
α'-C_2S	–	Mueller [13]
C_3A_{cubic}	1841	Mondal and Jeffery [14]
$C_3A_{orthorombic}$	100220	Takéuchi and Nishi [15]
C_4AF	51265	Jupe et al. [16]
Gypsum	27221	Pedersen [17]
Bassanite	380286	Weiss and Bräu [18]
Anhydrite	16382	Kirfel and Will [19]
Calcite	80869	Maslen et al. [20]
Quartz	174	Le Page and Donnay [21]
Arcanite	79777	Ojima et al. [22]
Ettringite	155395	Goetz-Neunhoeffer and Neubauer [23]
Portlandite	34241	Busing and Levy [24]
Silicon	51688	Többens et al. [36]

$$C_j = S_j\frac{\rho_j V_j^2 \mu_{SAMPLE}^*}{G} \quad (2)$$

The intensity caused by the Kapton polyimide film was fitted with a specific model. To this end, the Kapton film was stretched over a single crystal sample holder and the pattern of the Kapton film was fitted with a peaks phase, which was later implemented into the refinement of the cement paste [10]. All structure models used for the Rietveld refinement are shown in Table 3. Mass attenuation coefficients for the various elements were drawn from the International Tables for Crystallography [37]. The mass attenuation coefficient of the cement (97.95 cm^2/g) was calculated from its chemical composition. Mass attenuation coefficients of the cement pastes were calculated taking into account the composition of the paste (water, cement, polymer) and the respective mass absorption coefficients of all ingredients (water = 10.28 g/cm^2; PDADMAC ≈ 26.6 g/cm^2).

It was recently shown that the calculation of heat flow curves from XRD in situ data concords well with heat flow diagrams measured by heat flow experiments [4]. This approach indeed has many advantages when it comes to showing clearly where the influence of additives on the hydration process is visible.

To this end, Eq. (3) is assumed for the silicate reaction [45].

$$C_3S + 3.9H \rightarrow C_{1.7}SH_{2.6} + 1.3CH \quad \Delta H_R = -561\ J/g \quad (3)$$

The enthalpy of reaction was calculated using the enthalpy of formation of water from the GEMS version of the Nagra/PSI thermodynamic database [40]. The enthalpies of formation for alite and portlandite were taken from the cemdata07 database [41] and the data of Fuji and Kondo [42] for the enthalpy of formation for $C_{1.7}SH_{2.6}$.

The calculation of heat flow curves (HF) from XRD data generally follows Eq. (4) [4].

$$HF = \frac{\frac{\partial\ wt.\%\ phase}{\partial t}}{100} \times \Delta H_R \quad (4)$$

where $HF = \frac{\frac{\partial\ wt.\%\ phase}{\partial t}}{100} \times \Delta H_R$ is the derivative of the phase content curves and ΔH_R the enthalpy of reaction.

In the present research, heat flow curves were calculated for the silicate reaction alone, in order to illustrate particularly clearly the influence of the polymers used on the silicate reaction during hydration of the cement.

3. Results

Fig. 3 shows the measured heat flow curves of the cement used with and without addition of the substituted PDADMA. It can be seen that the different types of PDADMA affect the cement

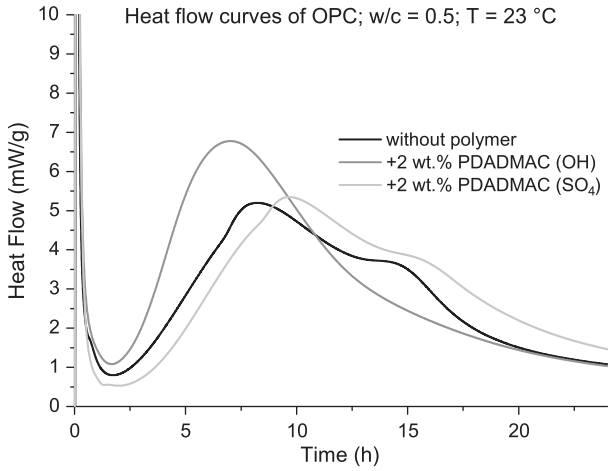

Fig. 3. Heat flow curves for the OPC used with and without polymer addition.

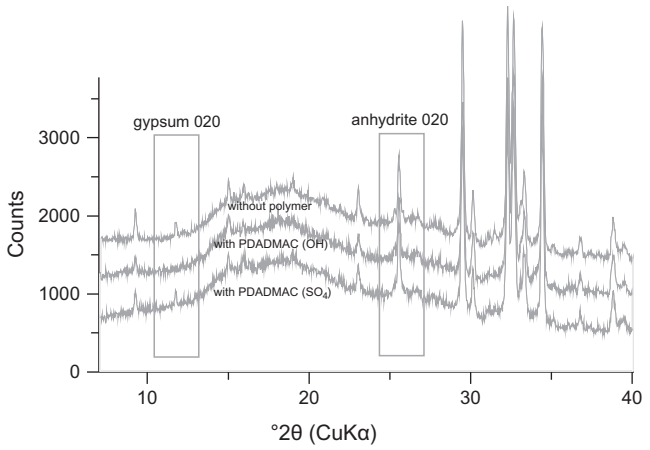

Fig. 5. First XRD patterns of the cement pastes recorded with and without polymer addition.

hydration in different ways. The OH^--substituted PDADMA causes an acceleration of the cement hydration. Where PDAMA (OH) is added, the two local heat flow maxima, which occur respectively at 8 h and 15 h after the start of hydration in the system without polymer added cannot be separated from each other, they seem to overlap. By contrast, the adding of SO_4^{2-}-substituted PDADMA produces a noticeable retardation of the cement hydration. Nevertheless, despite this retardation of the cement hydration, it can be seen in the heat flow diagrams that it is still possible to separate the two heat flow maxima from one another during the main reaction.

Fig. 4 shows the change of phase contents of C_3A, anhydrite and gypsum for all cement pastes examined (with and without polymer) within 22 h. It can be clearly seen that the polymers affect the dissolution of the phases, which react during the process of hydration in order to form the hydrate phase ettringite.

Where the OH^--substituted PDADMA is added, there is no gypsum detectable in the first XRD pattern of the cement paste (Fig. 5). In the system without polymer addition, and in the system where it is rather the SO_4^{2-}-substituted PDADMA that is added, there is the same amount of gypsum detectable in the first XRD pattern as was determined in the dry cement (concerning the w/c-ratio of 0.5).

The addition of the SO_4^{2-}-substituted PDADMA leads to a secondary gypsum precipitation during the first hours of hydration. The dissolution of the phase anhydrite begins, in the system with the OH^--substituted PDADMA, immediately after the mixing of the cement with the polymer–water mixture. In the other systems examined, there is also a dissolution of anhydrite detectable immediately after the beginning of hydration. However, this latter dissolution ceases at a point between 3 and 7 h, while the dissolution of gypsum continues to be detectable.

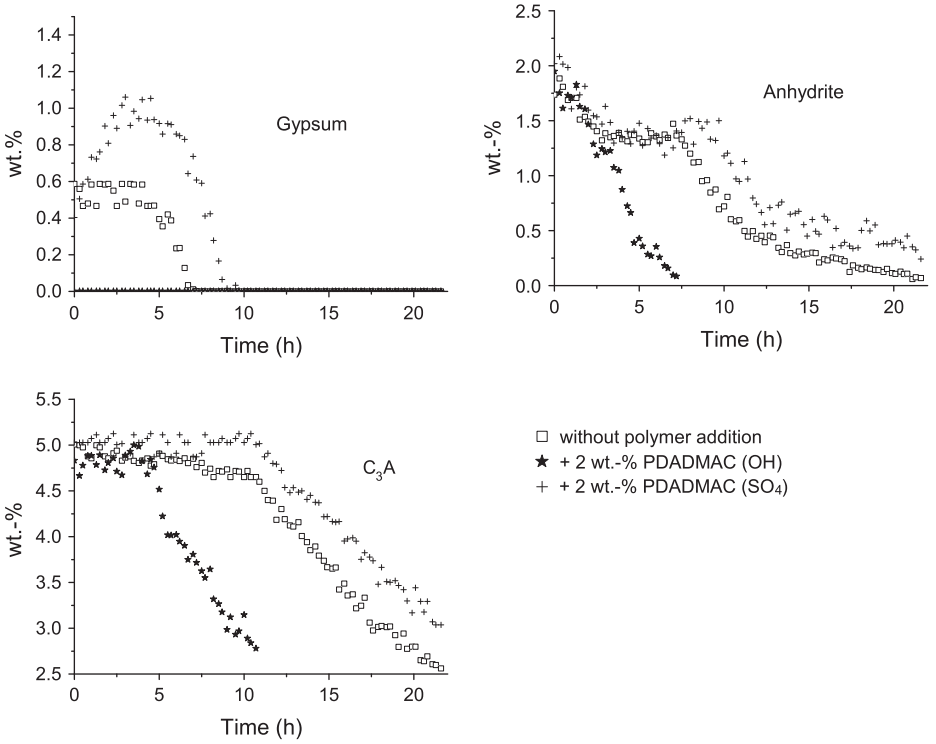

Fig. 4. Phase contents of gypsum (±0.1 wt.%), anhydrite (±0.2 wt.%) and C_3A (±0.5 wt.%) in the cement pastes with and without polymer addition.

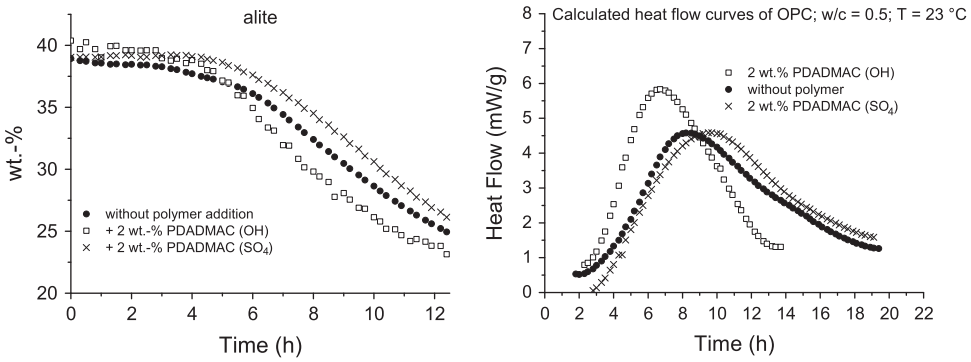

Fig. 6. Alite contents (±2 wt.%) in the cement pastes with and without addition of polymer (left side) and heat flow curves calculated from XRD data (right side).

In none of the systems examined did the C_3A dissolution begin before the dissolution of anhydrite, the last available sulfate carrier, was slowed down. Therefore, the dissolution of the C_3A in the system with OH^--substituted PDADMA occurs at least 5 h earlier than it does in either the system without addition of any polymer or the system with SO_4^{2-}-substituted PDADMA added.

Because of the secondary gypsum precipitation, sulfate carriers are available for a longer period in the cement paste with PDADMA (SO_4) and further dissolution of C_3A is delayed by higher SO_4^{2-} concentration in the pore solution.

The curves for the phase alite are shown in Fig. 6 (left side). It can be seen that the addition of 2 wt.% of PDADMAC (OH) causes a clear acceleration of the alite dissolution, while the addition of 2 wt.% of PDADMA (SO_4) causes a slight retardation of the alite dissolution in the cement paste. This fact can also be seen when comparing the heat flow curves calculated from XRD data (Fig. 6 right side).

4. Discussion

The phases which are involved in the aluminate reaction and that lead to the formation of ettringite react successively. It can be seen from the XRD data that the dissolution of C_3A does not occur synchronously with the dissolution of the sulfate carriers (Fig. 7). Moreover, the dissolution of the sulfate carriers in the cement paste also occurs successively. No synchronous dissolution of anhydrite and gypsum can be detected throughout the whole hydration process. The same can be observed when adding polymers to the cement paste. Neither in the cement paste with PDADMA (OH) added nor in the cement paste with PDADMA (SO_4) added does the C_3A begin to be dissolved at any point in time before a slowdown of the anhydrite dissolution can be detected (point c in Fig. 7). We attribute the slowdown of the dissolution to the effect of some last remaining larger particles of anhydrite, which cannot supply enough SO_4^{2-} into the pore solution. Thus, it can be

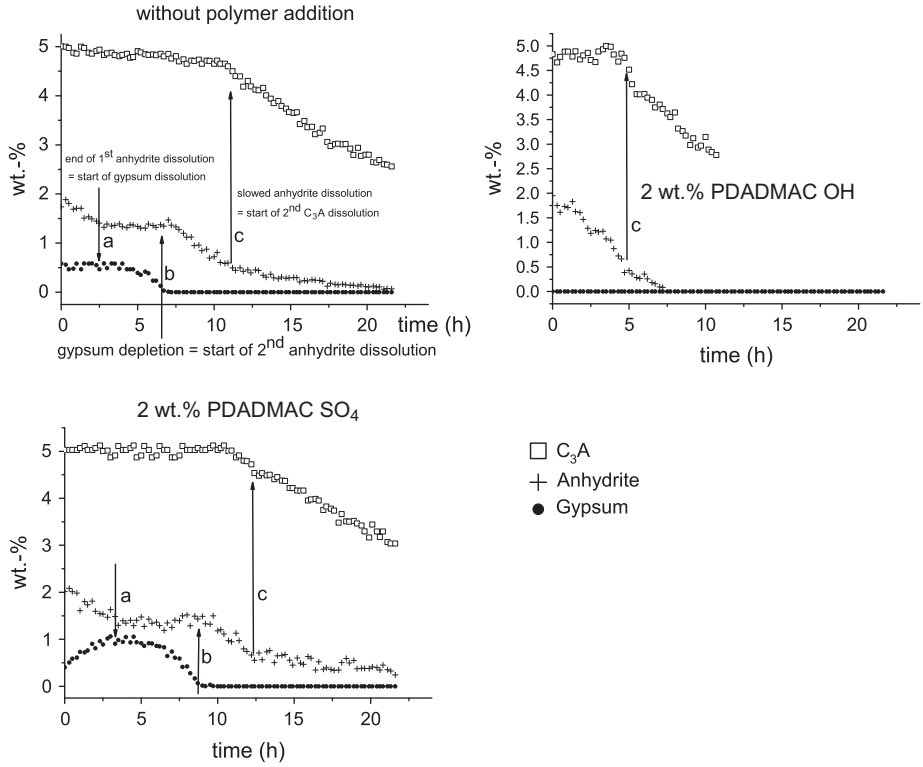

Fig. 7. Phase contents of C_3A (±0.5 wt.%), anhydrite (±0.2 wt.%) and gypsum (±0.1 wt.%) in the cement pastes with and without polymer addition.

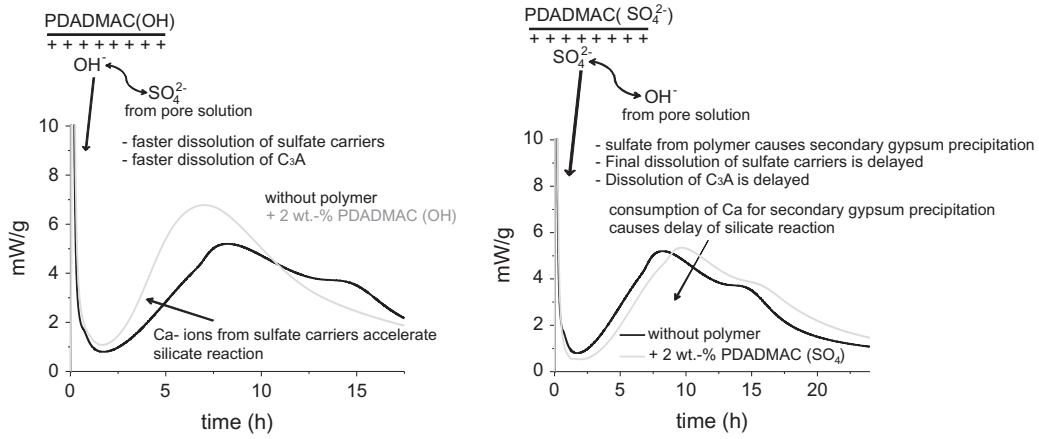

Fig. 8. Models for the influence of the different PDADMACs on the hydration of the OPC used in the study.

assumed that the dissolution of the C_3A is controlled by the presence of sulfate in the pore solution.

A specific amount of C_3A is immediately dissolved after mixing the cement with water. But as soon as the sulfate concentration of the pore solution is high enough the dissolution of C_3A is stopped until the last "available" sulfate carrier (in our case anhydrite) is dissolved or the dissolution is slowed down (which is very often the case in commercial cements due to a few coarse particles of anhydrite). Thus, it is likely that the presence of the sulfate carriers, or alternatively the sulfate concentration in the pore solution, suppresses the further dissolution of the C_3A [4,5].

The different influences exerted by the different polymers PDADMA (OH) and PDADMA (SO_4) can be explained as follows (Fig. 8): A rapid exchange between the OH– groups of the PDADMA (OH) and the sulfate ions from the pore solution causes a depletion of sulfate in the pore solution. Gypsum is dissolved immediately after mixing in order to adjust equilibrium between the pore solution and the solid. Thus, gypsum can no longer be detected in the first XRD pattern with PDADMA (OH) added (Fig. 5). Since there is no gypsum available in the cement paste, an immediate dissolution of anhydrite can be detected in the system with PDADMA (OH) added. After about 5 h, a retardation of the anhydrite dissolution causes the onset of further dissolution of the C_3A. The acceleration of the alite dissolution is a secondary effect of the rapid dissolution of the sulfate carriers. The rapid dissolution of the sulfate carriers causes a higher Ca^{2+} concentration in the pore solution and this in consequence may lead to an acceleration of the alite dissolution or of the silicate reaction respectively. The accelerating influence of Ca-providing compounds such as Ca-formate and $CaCl_2$ have been described very often [38] in construction chemistry. In the case of the PDADMA (OH) system the Ca-providing compound is the sulfate carrier of the cement. Another aspect which should be mentioned is the possibility that both polymers might have an impact on the pH-value of the cement paste. The PDADMA (OH) releases OH groups into the pore solution and might therefore increase the pH-value while the PDADMA (SO_4) might decrease the pH-value inasmuch as it takes away OH groups from the pore solution.

While the addition of the PDADMA (OH) leads to a more rapid dissolution of the sulfate carriers, C_3A and alite, the addition of the PDADMA (SO_4) causes a secondary gypsum formation during the first hours of hydration and retards the dissolution of the reactive phases C_3A and alite. The presence of an increased sulfate concentration in the pore solution can be traced back to an exchange occurring between SO_4^{2-} supplied by the polymer and OH^- ions from the pore solution. The formation of secondary gypsum, which can be detected with X-rays, leads to a depletion of Ca^{2+} in the pore solution, which in turn causes the prolongation of the induction period. The further dissolution of the C_3A is retarded because of the increased content of available SO_4^{2-}. Since there is more gypsum in the cement paste, the complete dissolution of the sulfate carriers takes more time than in the system without polymer added. The dissolution of gypsum is entirely completed after 7.5 h in the system without polymer added and at about 9 h in the system with PDADMA (SO_4) added (Fig. 7). Thus, the further dissolution of anhydrite is delayed leading to a further retardation of the C_3A dissolution. The second heat flow maximum, which can be ascribed to the dissolution of the C_3A and an accelerated ettringite precipitation, occurs at later points of time than in the system without polymer.

Finally, Fig. 9 shows the measured heat flow curves of all cement pastes examined, as well as the heat flow curves for the sil-

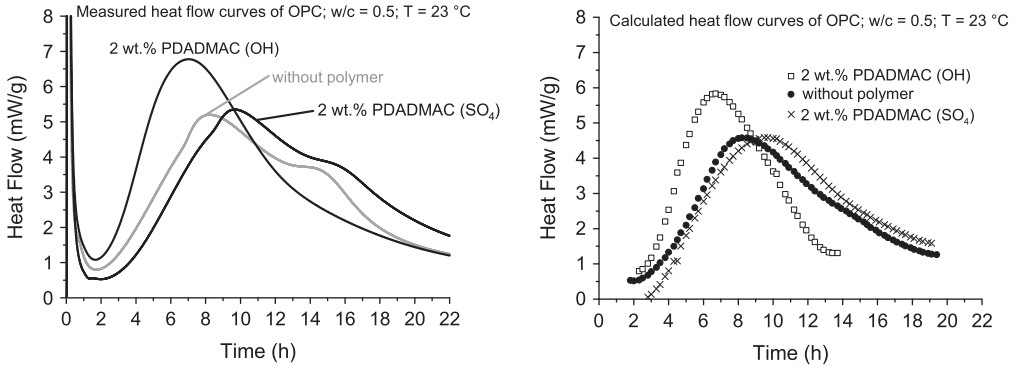

Fig. 9. Comparison between measured heat flow and the heat flow calculated from XRD data.

icate reaction as calculated from XRD data. The influence of the polymers on the alite dissolution (and C–S–H–, portlandite precipitation) can be clearly demonstrated. It can be seen that the PDADMA (OH) clearly accelerates the silicate reaction and that the PDADMA (SO_4) slightly retards the silicate reaction. It must be emphasized that the calculated heat flow curves do not include the heat released by the dissolution of C_3A, anhydrite, or gypsum, nor do they include the heat released during the precipitation of ettringite.

5. Conclusion

The phase development of cements during hydration can be traced by means of quantitative X-ray diffraction combined with heat flow calorimetry. This combination of methods could contribute to a better understanding about the influence of the investigated substituted PDADMA polymers on the silicate reaction of a commercial CEMI 52.5 R. The reported data suggest a distinct interaction in pore solution between ions from the substituted PDADMA and ions (e.g. Ca^{2+}, SO_4^{2-}, OH^-) released during cement hydration.

The observed acceleration of alite dissolution by addition of OH^- substituted PDADMA is only a secondary effect of the rapid dissolution of bassanite and gypsum. At very early times of hydration primarily an ion exchange between the OH^- groups of the PDADMA (OH) and the SO_4^{2-} ions from the pore solution takes place. The shortage of SO_4^{2-} in pore solution consequently accelerates dissolution of the calcium sulfates in the OPC leading to a higher concentration of Ca^{2+} in solution.

By contrast, the adding of SO_4^{2-}-substituted PDADMA produces a noticeable retardation of the dissolution of all reactive phases, especially alite and C_3A. In this case an ion exchange occurring between SO_4^{2-}, supplied by the polymer, and OH^- ions from the pore solution leads to an increase of available SO_4^{2-} in the pore solution. This delays dissolution of the C_3A, alite, anhydrite and as a consequence of this the precipitation of ettringite, C–S–H and portlandite. At the same time the increase in SO_4^{2-} in solution will decrease the Ca^{2+} content and is responsible for the retardation of the silicate reaction.

References

[1] Bayer R, Lutz H. Dry mortars, Ullmann's encyclopedia of industrial chemistry; 2009.
[2] Juilland P, Gallucci E, Flatt R, Scrivener K. Dissolution theory applied to the induction period in alite hydration. Cem Concr Res 2010;40:831–44.
[3] Bullard JW, Jennings HM, Livingston RA, Nonat A, Scherer GW, Schweitzer JS, et al. Mechanisms of cement hydration. Cem Concr Res 2011;41:1208–23.
[4] Hesse C, Goetz-Neunhoeffer F, Neubauer J. A new approach in quantitative in-situ XRD of cement pastes: correlation of heat flow curves with early hydration reactions. Cem Concr Res 2010;41:123–8.
[5] Jansen D, Goetz-Neunhoeffer F, Stabler Ch, Neubauer J. A remastered external standard method applied to the quantification of early OPC hydration. Cem Concr Res 2001;41:602–8.
[6] Schorm A, Weitzel HP, Killat S, Lutz H. Wacker Chemie AG. EP 1984 428.
[7] O'Connor BH, Raven MD. Application of the rietveld refinement procedure in assaying powdered mixtures. Powder Diffr 1988;3:2–6.
[8] Jansen D, Stabler Ch, Goetz-Neunhoeffer F, Dittrich S, Neubauer J. Does Ordinary Portland Cement contain amorphous phase? A quantitative study using an external standard method. Powder Diffr 2011;26:31–8.
[9] Rietveld HM. A profile refinement method for nuclear and magnetic structures. J Appl Crystallogr 1969;2:65–71.
[10] Hesse C, Goetz-Neunhoeffer F, Neubauer J, Braeu M, Gaeberlein P. Quantitative in situ X-ray diffraction analysis of early hydration of Portland cement at defined temperatures. Powder Diffr 2009;24:112–5.
[11] De La Torre AG, Bruque S, Campo J, Aranda MAG. The superstructure of C_3S from synchrotron and neutron powder diffraction and its role in quantitative phase analysis. Cem Concr Res 2002;32:1347–56.
[12] Jost KH, Ziemer B, Seydel R. Redetermination of the structure of β-dicalcium silicate. Acta Crystallogr, Sect B: Struct Crystallogr Cryst Chem 1977;33:1696–700.
[13] Mueller R. Stabilisierung verschiedener Dicalciumsilikat-Modifikationen durch den Einbau von Phosphat: Synthese, Rietveldanalyse, Kalorimetrie. Diploma Thesis. University of Erlangen; 2001.
[14] Mondal P, Jeffery J. The crystal structure of tricalcium aluminate, $Ca_3Al_2O_6$. Acta Crystallogr, Sect B: Struct Crystallogr Cryst Chem 1975;31:689–97.
[15] Takéuchi Y, Nishi F. Crystal-chemical characterization of the Al_2O_3–Na_2O solid-solution series. Z Kristallogr 1980;152:259–307.
[16] Jupe AC, Cockcroft JK, Barnes P, Colston SL, Sankar G, Hall C. The site occupancy of Mg in the brownmillerite structure and its effect on hydration properties: an X-ray/neutron diffraction and EXAFS study. J Appl Crystallogr 2001;34:55–61.
[17] Pedersen BF. Neutron diffraction refinement of the structure of gypsum. Acta Crystallogr, Sect B, Struct Crystallogr Cryst Chem 1982;38:1074–7.
[18] Weiss H, Bräu MF. How much water does calcined gypsum contain? Angew Chem Int Ed 2009;48:3520–4.
[19] Kirfel A, Will G. Charge density in anhydrite $CaSO_4$, from X-ray and neutron diffraction measurements. Acta Crystallogr, Sect B: Struct Crystallogr Cryst Chem 1980;36:288–2890.
[20] Maslen EN, Streltsov VA, Streltsova NR. Electron density and optical anisotropy in rhombohedral carbonates. III. Synchroton X-ray studies of $CaCO_3$, $MgCO_3$ and $MnCO_3$. Acta Crystallogr, Sect B: Struct Sci 1995;51:929–39.
[21] Le Page Y, Donnay G. Refinement of the crystal structure of low-quartz. Acta Crystallogr, Sect.B: Struct Crystallogr Cryst Chem 1976;32:2456–9.
[22] Ojima K, Hishihata Y, Sawada A. Structure of potassium sulfate at temperatures from 296 K down to 15 K. Acta Crystallogr, Sect B: Struct Sci 1995;51:287–93.
[23] Goetz-Neunhoeffer F, Neubauer J. Refined ettringite structure for quantitative X-ray diffraction analysis. Powder Diffr 2006;21:4–11.
[24] Busing WR, Levy HA. Neutron diffraction study of calcium hydroxide. Acta Crystallogr, Sect B: Struct Sci 1986;42:51–5.
[25] Lerch W. The influence of gypsum on the hydration and properties of Portland cementpastes. Am Soc Test Mater 1946;46:1252–97.
[26] Plank J, Gretz M. Study on the interaction between anionic and cationic latex particles and Portland cement, Colloids and Surfaces A: Physicochem. Colloids Surf 2008;330:227–33.
[27] Plank J, Chatziagorastou P, Hirsch C. New model describing distribution of adsorbed superplasticizer on the surface of hydrating cement grain. J Build Mater 2007;10:7–13.
[28] Larbi JA, Bijen J. Interaction of polymers with Portland cement during hydration – a study of the chemistry of the pore solution of polymer-modified cement systems. Cem Concr Res 1990;20:139–47.
[29] Su Z, Bijen JMJM, Larbi JA. Influence of polymer modification on the hydration of Portland cement. Cem Concr Res 1991;21:242–50.
[30] Chandra S, Flodin P. Interactions of polymers and organic admixtures on Portland cement hydration. Cem Concr Res 1987;17:875–90.
[31] Silva DA, Roman HR, Gleize PJP. Evidences of chemical interaction between EVA and hydrating Portland cement. Cem Concr Res 2002;32:1383–90.
[32] Silva DA, Monteiro PJM. Analysis of C_3A hydration using soft X-rays transmission microscopy: effect of EVA copolymer. Cem Concr Res 2005;35:2026–32.
[33] Silva DA, M Monteiro PJ. Hydration evolution of C3S-EVA composites analyzed by soft X-ray microscopy. Cem Concr Res 2005;35:351–7.
[34] Silva DA, Monteiro PJM. The influence of polymers on the hydration of Portland cement phases analyzed by soft X-ray transmission microscopy. Cem Concr Res 2006;36:1501–7.
[35] Dimmig-Osburg A, Pietsch I, Pakusch J. Polymer additives and their influence on the cement microstructure in the early stages of hardening. ZKG Int 2006;59:72–83.
[36] Többens DM, Stuesser N, Knorr K, Mayer HM, Lampert G. The new high-resolution neutron powder diffractometer at the Berlin neutron scattering center. Mater Sci Forum 2001;378–381:288–93.
[37] E. Prince, editor. International Union for Crystallography, International Tables for Crystallography, Volume C: mathematical, physical and chemical tables. 3rd ed. Boston: Kluwer; 2004.
[38] Dodson V. Concrete admixtures, structural engineering series. New York: Van Nostrand Reinhold; 1990.
[39] Cheary RW, Coelho A. A fundamental parameters approach to X-ray line-profile fitting. J Appl Cryst 1992;25:109–21.
[40] Hummel W, Berner U, Curti E, Pearson FJ, Thoenen T. Nagra/PSI Chemical Thermodynamic Data Base 01/01. USA, also published as Nagra Technical Report NTB 02-16, Wettingen, Switzerland. Universal Publishers/uPUBLISH.com; 2002. p. 565.
[41] Lothenbach B, Matschei T, Möschner G, Glasser FP. Thermodynamic modeling of the effect of temperature on the hydration and porosity of Portland cement. Cem Concr Res 2008;38(1):1–18.
[42] Fuji K, Kondo W. Communications of the American ceramic society: estimation of thermochemical data for calcium silicate hydrate (C–S–H). J Am Ceram Soc 1983;66:C-220–1.
[43] Bishnoi S, Scrivener KL. Studying nucleation and growth kinetics of alite hydration using μic. Cem Concr Res 2009;39:849–60.
[44] Thomas JJ. A new approach to modeling the nucleation and growth kinetics of tricalcium silicate hydration. J Am Ceram Soc 2007;90:3282–8.
[45] Allen AJ, Thomas JJ, Jennings HM. Composition and density of nanoscale calcium–silicate–hydrate in cement. Nat Mater 2007;6:311–6.